

High-Resolution Three-Dimensional Whole-Organ Tomography of Microbial Infections

Jiagui Li¹, Alaa Alhayek¹, Heng Wang¹, Dirk Bumann¹

¹ Biozentrum, University of Basel

Corresponding Author

Dirk Bumann

dirk.bumann@unibas.ch

Citation

Li, J., Alhayek, A., Wang, H., Bumann, D. High-Resolution Three-Dimensional Whole-Organ Tomography of Microbial Infections. *J. Vis. Exp.* (205), e66469, doi:10.3791/66469 (2024).

Date Published

March 1, 2024

DOI

10.3791/66469

URL

jove.com/video/66469

Abstract

Most infections take place within three-dimensional host tissues with intricate anatomy and locally varying host physiology. The positioning of pathogen cells within this diverse environment significantly affects their stress levels, responses, fate, and contribution to the overall progression of the disease and treatment failure. However, due to the technical difficulties in locating μm -sized pathogen cells within cm -sized host organs, this area of research has been relatively unexplored. Here, we present a method for addressing this challenge. We employ serial two-photon tomography and AI-enhanced image analysis to locate individual *Salmonella* cells throughout the entire spleen, liver lobes, and whole lymph nodes of infected mice. Using fluorescent reporters and *in vivo* antibody administration, the replication rate of single *Salmonella* cells, their local interaction with specific immune cells, and bacterial responses to antibiotics can be determined. These methodologies open avenues for a comprehensive examination of infections, their prevention, and treatment within the three-dimensional tissue context.

Introduction

Infections occur in tissues with complex anatomy and compartmentalized physiology. The diverse microenvironments that co-exist in the infected tissue can determine the fates of local pathogen subsets and their contributions to overall disease outcome^{1,2,3}. However, comprehensive 3D mapping of microbial pathogens in cm -sized tissues remains challenging⁴. Imaging of the brain and other organs is a highly active research field with constantly improving experimental strategies⁵, but many methods still lack the sub- μm resolution that would be required to identify

μm -sized bacterial pathogens confidently. In contrast, serial two-photon (STP) tomography⁶ enables automated multi-color, deformation-free imaging of entire tissues with sub- μm in-plane resolution, yielding full volumetric datasets. This method combines repeated physical sectioning of the tissue using a vibratome with intermittent two-photon imaging of the emerging block faces with infrared light. STP tomography has been widely used for mapping thin axons in the brain to establish connectivity maps^{7,8,9,10}.

STP tomography also enables 3D mapping of individual microbial pathogen cells (*Salmonella*, *Toxoplasma*) in the entire infected tissues^{11,12} using a tomograph. Second-harmonic generation reveals collagen sheaths around arteries and in fibrous bands such as the trabeculae of spleen, thus providing anatomical context. *In vivo* injected fluorescent antibodies can be used to stain host cells to reveal interactions between individual pathogen cells and infiltrating immune cells such as neutrophils. Here, the pipeline involving processing of the tissue, imaging, stitching of imaging tiles with illumination correction, stacking of images in three dimensions, and segmentation using machine-learning tools, is described. This pipeline yields 3D positions of individual pathogens cells and microcolonies within their host context. Counting the number of individual cells within microcolonies remains difficult because of resolution limits, but such numbers can be estimated based on the integrated brightness of the microcolony. The pipeline can be readily adapted to other infection models if recombinant GFP- or YFP-expressing pathogens are available.

Protocol

All animal experiments described here have been approved by the authorities (license 2239, Kantonales Veterinäramt Basel) and follow local guidelines (Tierschutz-Verordnung, Basel) and the Swiss animal protection law (Tierschutz-Gesetz).

1. Preparation and storage of infected tissues

1. Use an infection model of choice. Here, 10 to 16 weeks-old mice of both sexes are infected with ~1,000 colony-forming units (CFU) by intravenous injection or 5×10^7 CFU by intragastric administration with a round-

tip needle. Suitable mouse strains include BALB/c and C57BL/6.

NOTE: The same approach can be easily adapted for other host species.

2. Ensure pathogens express fluorescent proteins for enabling identification in unstained tissue. Pathogens expressing GFP.mut2¹³, YPet¹⁴, TIMER^{bac15}, or mWasabi¹⁶ can all be visualized using 940 nm excitation¹⁷. *Salmonella* expressing mCherry¹⁸ at levels readily detectable by flow cytometry¹⁹ could be imaged using 800 nm excitation but have poor signal-to-background ratios in infected spleen and liver which show substantial autofluorescence.
3. Ensure all the fluorescent proteins retain >70% of their fluorescence intensity after fixation with paraformaldehyde at neutral pH based on quantification with flow cytometry. Here, infected mouse tissue, namely, spleen, liver, lymph nodes, and Peyer's patches are used.
4. Stain host cell surface markers *in vivo* by injecting phycoerythrin (PE)-labeled antibodies 10 min prior to perfusion. To stain neutrophils, inject intravenously 4 µg anti-Ly-6G-PE in 100 µL of PBS. To stain marginal zone macrophages in the spleen, inject 4 µg anti-CD169-PE in 100 µL of PBS (see **Table of Materials**).
5. Fix infected tissues through standard transcardial perfusion²⁰ with 15 mL of ice-cold 50 mM phosphate buffer (PB; 10 mM NaH₂PO₄, 40 mM Na₂HPO₄, pH 7.4), followed by 35 mL of 4% paraformaldehyde (PFA; fixative) in PB (**Figure 1A**).
 1. In brief, administer deep anesthesia to the infected animal by intraperitoneal injection of 100 mg/kg

ketamine and 16 mg/kg xylazine. Ensure proper anesthetization by confirming loss of the toe-pinch reflex.

2. Disinfect the fur using 70% ethanol, dry it with a sterile paper towel, and surgically open the chest with tweezers and scissors. Place a sterile needle in the left ventricle of the heart, open the right atrium with sterile scissors, and run the first buffer and then fixative through the needle, the left ventricle, and the entire vascular system using a pump. This fixes all tissues rapidly and uniformly and causes euthanasia.
6. Collect the tissue after perfusion, incubate it in 20x volume of 4% cold paraformaldehyde in PB buffer and place it on a shaker at 4 °C overnight (**Figure 1B**). Imaging is possible for tissues in the size range of 0.05 to 2 cm³. For larger tissues, cut into suitable pieces.
7. The next day, wash the tissue 3x for 10 min each with PB buffer with shaking at 40 rpm at room temperature to remove PFA.

NOTE: Because of PFA toxicity, these steps must be carried out inside a fume hood. Dispose of the PFA waste according to institutional guidelines.
8. Remove any excess PB buffer and add 20x volume of cryoprotectant storage buffer²¹ (876 mM sucrose, 0.25 mM polyvinylpyrrolidone, 40% (v/v) ethylene glycol, dissolved in 50 mM PB buffer) to the sample with shaking at 40 rpm at 4 °C for 6-8 h or until the tissues sink to the bottom. Incubate samples at -20 °C for at least 3 days to ensure effective reduction of tissue autofluorescence¹¹. Samples can be used for up to 5 years when stored at -20 °C.

NOTE: The sinking of the tissue indicates proper penetration of the storage buffer into the tissue.

2. Sample embedding

1. Embed the tissue into an agarose block for smooth cutting with a vibratome. Pre-activate the agarose chemically by oxidation with periodate and then reduce with borohydride to form cross-link with the tissue for improved stability during the cutting process. Perform the steps described below.
2. Prepare 4% oxidized agarose by weighing 2.25 g agarose and add 0.21 g NaIO₄. Add 100 mL of PB to the agarose and NaIO₄. Stir at room temperature in a fume hood for 2-3 h with protection from light.

NOTE: Critical step: Do not exceed stirring for more than 3 h or the agarose will polymerize poorly.
3. Recover the agarose by membrane filtration in a standard vacuum filter with a 0.2 µm membrane. Remove remaining NaIO₄ by washing 3x with 50 mL of PB buffer. Resuspend the oxidized agarose in 50 mL of PB buffer.

NOTE: Do not melt the agarose during this stage. The agarose can be stored at 4 °C for up to 2-3 weeks protected from light.
4. Prepare borohydride solution by adding 19 g borax and 3 g boric acid to 1 L of water. Stir until dissolved and adjust the pH to 9-9.5 with 1 M NaOH. On a stirring plate in a fume hood, heat 100 mL of borate buffer to 40 °C. Add 0.2 g NaBH₄ and stir for 15-30 min while protecting from light.

NOTE: The borohydride solution can be stored for several weeks at room temperature in the dark. Critical step: When adding NaBH₄ to the borate buffer, gas will be formed, therefore conduct this step inside a fume hood.

Do not do this step in a tightly sealed container because it might lead to an explosion.

5. Take tissue from the freezer after sufficient incubation for reduced autofluorescence (≥ 3 days), remove excess cryoprotectant storage buffer, and wash the tissue 3x for 10 min each with PB buffer with shaking at 40 rpm at room temperature (RT).
6. Melt approximately 20 mL of oxidized agarose suspension (prepared in step 1) in a microwave (700 W for ~ 30 s), allow it to cool enough to handle (~ 45 °C), and pour it into a plastic mold.
NOTE: Critical step: Do not add the agarose directly after heating it up in the microwave on the sample, this might lead to destroying the tissue.
7. Use a tweezer to gently pick up the tissue and insert it quickly into the bottom center of the agarose. Incubate the mold at RT for 15 min to allow the agarose to polymerize.
8. Following agarose polymerization, open the plastic mold with a scalpel from its four corners and carefully pick up the agarose cube with gloved fingers.
9. Immerse the sample in borohydride solution (prepared in step 2) for 2-3 h at 4 °C to initiate cross-linking of the oxidized agarose and the tissue. This prevents the tissue from detaching during sectioning.
NOTE: Critical step: The immersed sample in borohydride should be incubated protected from light at 4 °C.
10. Wash the agarose cube with PB buffer 2x for 10 min. Turn the agarose cube so that the tissue is at the upper side and attach the block to a magnetic slide (microscope slide with two magnets attached to the back) using a few drops of instant adhesive. It takes 10-20 min for the glue

to solidify, so place a paper tissue with drops of PB buffer on top of the agarose ensuring that the sample remains adequately hydrated throughout (**Figure 1C**).

3. Preparation of the microtome and setting the stage

1. Place the magnetic slide on the metal in the center of the sample box of the tomograph.
2. Fill the box with PB buffer and carefully position it on the stage and tighten the screw on the left to secure the sample box on the stage of the tomograph.
NOTE: Do not over-tighten the screws, or it will damage the plastic box.
3. Place the blade on the microtome and shift the position of the sample carefully near and underneath the microtome. The upper surface of the agarose should be at the same level as the blade of the microtome.
NOTE: Positioning it too low will waste cutting time, while positioning it too high will remove a large chunk of the block at the first cut.
4. Move the stage to position the agarose cube to the center of the objective and click repeatedly on **Slice** button in the tomograph software until you get an intact slice of the entire agarose cube.

4. Allocation of the surface and acquiring 2D images

1. Center the objective lens on the tissue sample in x- and y-directions.
2. Open the laser software and turn on the laser in the software. Upon hearing a ticking sound, turn the laser switch on, and adjust the wavelength to 800 nm.
NOTE: The laser source needs to be warmed up for at least 30 min, ideally 1 h, before imaging.

- Close the cabinet doors of the microscope, switch off all light sources in the room, and turn on the PMTs and set the voltage to 750 V.

NOTE: Critical step: PMTs are very sensitive to light, keep it off unless the cabinet doors are closed and all the light sources in the room are turned off.

- Adjust the protocol settings of the tomograph software as outlined and set the microscope shutter to automatic and the voltage to 20 and 3 for V1 and V2, respectively.
- Click on the **2D button** in tomograph software to capture a snap of the sample.
- Once an image with visible autofluorescence appears, adjust the z-piezo to set the focal plane on the agarose cube surface. The first scan will be 20 μm under the surface to acquire a stable image of the sample.
 - If no autofluorescence background is visible, increase the contrast until a signal appears. It can occur that there is no visible signal (i.e., because of the agarose on top of the tissue). In this case, adjust the z-axis using the z-piezo device until it reaches the agarose surface. Manual movement of the lens may be needed if the desired position is outside of the range of the z-piezo device.
- Cut multiple 50 μm slices after finding the surface of the sample and acquire 2D images after every cut to make sure the focal plane is properly set on the block-face surface.

5. Finding the edges of the samples and setting the laser to the starting point

- Based on the xy-coordinates of the laser scan area (4 corner coordinates), confine the imaging area to the

tissue with minimal imaging of the surrounding agarose block.

- Turn off the PMTs, set the laser wavelength to 800 nm, switch the laser shutter to open. The position of laser light entering the agarose block is visible as a red spot of scattered light (**Figure 2A,B**).

Critical step: Be particularly careful with the class 4 laser. It can rapidly damage human tissues and eyes. Staff need special training to operate such an instrument safely.

- Use the laser spot while shifting the stage to find the coordinates of the tissue edges using the sequence back, right, front, and left.
- Double-check the coordinates and position the laser spot at the right-front corner, which is the default starting point for imaging the tissue.
- Convert the coordinates from the console window into machine-recognizable block sizes, which are defined by the xy-steps. Enter these step measurements into the protocol of the software. Close the cabinet doors.

6. 3D scanning / sectioning

- Change the wavelength to 940 nm to excite GFP, mWasabi, or YPet, and PE.

NOTE: The laser is invisible to the human eye at this wavelength. To enhance signal-to-background for GFP, mWasabi, and the green emitting component of TIMER^{bac}, put a narrow band-pass filter 510/20 nm in front of PMT 2. This reduces interference by green-yellow tissue autofluorescence.

- Switch the microscope shutter to automatic mode, and the shutter voltage settings to 20 for V1 and 1.71 for V2.

3. Adjust the following three parameters in the software: Section thickness- for most purposes, set to 50 μm . For liver, set to 30 μm because of limited imaging depth. The number of physical sections- this determines the total tissue depth that will be imaged, set accordingly. The number of planes to capture for each section -this will determine the z resolution. Use 5 planes (yielding 10 μm vertical resolution) for most purposes. For liver use 3 or less planes.
4. Set the laser gain. This needs to be empirically tested for different tissues and scanning depth.
5. Define the folder path and name for storing the acquired images and provide appropriate information for the imaging metafile.
6. Double-check all the entered values.
7. Click on **3D mosaic setting** to initiate the scanning process (**Figure 1D**).
8. After imaging is completed, carefully collect the tissue sections from the water tank and store them in storage buffer at $-20\text{ }^{\circ}\text{C}$ until further use (**Figure 1E**; **Figure 2C,D**).

7. Image processing and data analysis

1. Download the MATLAB scripts on a Linux computer from https://github.com/BumannLab/Li_BumannLab_2020. Copy the scripts to a folder, e.g., /home/user/Program/.
NOTE: The Computer Vision Toolbox add-on for MATLAB and Fiji (or ImageJ) must be installed on Linux computers for the script to be fully functional.
2. Stitch tile images as described below.

1. Transfer data from the tomograph server to the Linux computer.
 2. Open the MATLAB script StepOneStitchingAndArchive.m and locate the source folder containing the raw data. Define the source and destination folders in the script.
 3. Switch to the Editor tab and click **Run**. Progress information is displayed in the command window. The processing includes reading information from the Mosaic file, generating tile index before image stitching, background illumination correction with Cidre²² (**Figure 3**) as well as illumination correction between optical layers acquired at different depth. Find the stitched images in a subfolder called stitchedImages_100 in the source folder. Compress the raw data for long term storage using the tar command and save as a single file with the filename extension tar.bz2 (**Figure 1F**).
3. Perform model training and segmentation with support vector machine. To train the support vector machine and perform the segmentation follow the steps below.
NOTE: The stitched images for each of the three fluorescence channels are stored in 3 subfolders (named 1, 2, and 3, corresponding to red, orange, and green fluorescence) of stitchedImages_100. Each subfolder contains all the stitched images from the same channel.
 1. Preview the stitched images. Open one image with the same filename from each sub-folder with Fiji (or ImageJ). Merge the three channels into one color image. Adjust the brightness of each channel until clear signals are seen from bacteria and tissue autofluorescence. Note the adjusted

maximum intensity level of each channel for the next step.

2. Open the MATLAB script StepTwoSegmentationAndAnalysis.m and browse to source. Define the source folder and the image names for training. For example,


```
sourceD = '/';
red_name = [sourceD '1/section_020_01.tif'];
green_name = [sourceD '2/section_020_01.tif'];
blue_name = [sourceD '3/section_020_01.tif'];
```
3. Go to the Editor tab and click **Run**.
4. A dialogue box asking for color thresholds will appear, fill it based on previous manual check with Fiji (step 7.3.1).
5. Select regions for background and regions of interest (i.e., bacteria) according to the dialogs. Graphs will appear showing how well the model has been trained and asking if more regions need to be added. Add more regions of interest and background until the bacteria can be clearly segmented (**Figure 4A,B**).
6. Name and save the model. The script will automatically load the images and apply a median filter (radius 2 pixels).
7. The segmentation process automatically runs, and progress information is shown in the command window. Watch the progress of the segmentation. If the segmentation does not work well with the model on other stitched images, repeat the model training to include more background and bacterial regions.
8. To see the results of the segmentation, check the file named Allpositions_filter3D.txt. This file contains the coordinates of the center of gravity

for each bacterium or bacterial microcolony and the corresponding integrated fluorescence intensity (**Figure 1G**).

4. Remove additional artifacts with convolutional neural network as described below.

NOTE: For some bacteria, simple segmentation with the Support Vector Machine still includes some imaging artifacts. This is particularly true for YPet-expressing bacteria. Neural network-based segmentation can efficiently remove these artifacts (**Figure 4C**). The Computer Vision Toolbox add-on for MATLAB and Fiji (or ImageJ) must be installed on Windows computers for the script to be fully functional. For information on the underlying neural network see: <https://ch.mathworks.com/help/deeplearning/ug/create-simple-deep-learning-network-for-classification.html>

1. Prepare the images. Convert tif files to jpg files with different brightness adjustments using Fiji. Identify with manual curation at least 600 bacteria and 600 artifacts and save cropped images of these objects in appropriate folders.
2. Open the MATLAB script CNNtestV4.m and browse to the source files containing the object images of step 7.4.1.
3. Define the image folder for training. For example,


```
digitDatasetPath = fullfile ('D:\20200602_CNN','fortrainingPixel12Folder2');
```

 Define the number of images for training, e.g.,


```
numTrainFiles = 600.
```
4. Go to the Editor tab and click **Run**. After training, the CNN model file is saved as gregnet1.mat in the source folder.

5. Define a folder with test images. For example,


```
digitDatasetPathTest = fullfile('D:\20200602_CNN
\fortrainingPixel12Folder2\R2500G550B450yfp').
```

 The results are saved in a file YourFile.txt which contains information about the image name and the classification as bacteria or artifact.
6. Define folder with test images. For example,


```
digitDatasetPathTest = fullfile('D:\20200602_CNN
\fortrainingPixel12Folder2\R2500G550B450yfp').
```

 The results will be saved in a file YourFile.txt, which contains information about the image name and the classification as bacteria or artifact.
5. Estimate the size of micro-colonies based on fluorescence intensity of single bacteria as described below.

NOTE: The spatial resolution of the tomograph is insufficient to resolve individual bacterial cells within densely packed microcolonies. However, the number of bacteria in each microcolony can be estimated based on the total fluorescence of the microcolony in relation to the fluorescence of single bacteria. This estimation accuracy depends on the homogeneity of fluorescence intensity across the bacterial population.

 1. Confirm the identity of GFP-positive events in the STP tomography by staining bacterial components such as lipopolysaccharide using immunohistochemistry of retrieved sections from the tomograph (**Figure 1H**; **Figure 5**).
 2. Identify at least 30 single bacteria and retrieve their fluorescence intensity from the corresponding segmentation results. Utilize the median intensity value as reference for a single bacterium. Calculate the bacterial number of each microcolony by dividing the total fluorescence intensity of the microcolony by the reference value for a single bacterium (**Figure 1I**).
6. Perform 3D reconstruction with visualization software as described below.
 1. Image preparation
 1. Take the blue channel images, which contain second harmonic signals of collagen providing a useful anatomical reference including tissue capsules, arteries, and trabeculae. Use images segmented for bacteria as the 2nd channel.
 2. Bin down the images from 1st channel 10-fold in both x- and y-axes and save the downsized images in a new folder. Make 3 replicates of downsized images within the same folder. The name of new replicates should keep the same sequence. For example: section_001_01.tif, replicate 1 with name section_001_01-copy.tif, section_001_01-copy-copy.tif. Apply these steps also to the images from 2nd channel. The downsizing yields more manageable file sizes. The triple images will smoothen the z-axis.
 3. Merge the images from each channel to form image stacks with Fiji. Click **Image > Stacks > Tools > Stack sorter > Sort by labels**.
 4. Perform 3D filtering. Click **Process > Filters > 3D filter** and set Z filter size as 6. Save the image stacks.
 2. Perform 3D visualization as described below.
 1. Open the visualization software package in the Arena view (default setting). Use the Watch

- folder icon to add folders to the Arena view. Double click to open the *.ims or *.tif file (prepared in 7.6.1).
- Using **Edit>Image Properties**, adjust the color representations (LUTs) of the different channels in the Display Adjustment window.
 - Click on **Advanced** to manually set the min/max values and a value for gamma correction. Click on the **Channel names** to change the names and LUTs.
 - After adjusting the appearance of the image, export the current view using the Snapshot tool.
 - Use the Animation icon to represent the 3D data as a movie. Use the Navigation Pointer to find a perspective/view and zoom and use + Add to add keyframes. Move to another position and add the next keyframe. Press the **Red record** button to build the movie. Save it at the desired destination folder and file type (**Figure 1J**).

Representative Results

The described procedure enables detection of individual *Salmonella* cells in entire mouse organs such as spleen, liver, mesenteric lymph nodes, and Peyer's patches¹¹ (**Figure 5** and **Figure 6**). It also detects *Toxoplasma gondii* parasites in mouse brain¹². Some infected tissues including liver, Peyer's patches, and spleen emit substantial autofluorescence in the green-yellow range. Autofluorescence is further enhanced by the fixation with paraformaldehyde, which is necessary to preserve the tissue structure. Detection of green fluorescence from GFP, mWasabi, and the green component of TIMER^{bac} against this autofluorescence background is improved by putting a narrow bandpass filter 510/20 nm (transmitting

most GFP emissions but blocking a large part of the autofluorescence spectrum) in front of photomultiplier 2 (which collects green emissions) and by reducing tissue autofluorescence by storing fixed tissues for 3 or more days in cryoprotectant¹¹. However, bacteria should still express at least a few thousand copies per cell of GFP or other fluorescent proteins. On the other hand, excessive fluorescent protein levels should be avoided to minimize fitness costs that could lead to attenuated virulence²³.

Correct segmentation of fluorescent bacteria in the tissues can be confirmed by immunohistochemistry of retrieved tissue sections after imaging. Specifically, objects stained with an antibody to bacterial surface components such as lipopolysaccharide can be aligned with the fluorescence image obtained by STP tomography (**Figure 5**). It is important to note that some stained *Salmonella* cells lack fluorescent proteins and thus detectable fluorescence in both confocal microscopy and STP tomography. These cells are *Salmonella* that have been killed by the host immune system as demonstrated by flow cytometric sorting and growth cultures from single sorted cells as well as the close correlation between the number of colony-forming units on agar plates and the number of fluorescent *Salmonella* cells as determined by flow cytometry²⁴. In addition, plasmid loss can result in non-fluorescent viable cells and this needs to be tested by plating on media with and without appropriate antibiotics corresponding to the selection marker on the plasmid. For pSC101-derived plasmids, plasmid loss *in vivo* is rare¹⁹. For most chromosomally integrated expression cassettes such as *sifB::gfp* used in¹¹, loss of expression is undetectable *in vivo*. If the segmentation is inconsistent with immunohistochemistry data, the segmentation pipeline needs to be modified.

The resolution of STP tomography is insufficient to resolve individual bacterial cells within densely packed microcolonies. However, the total fluorescence intensity of the microcolony enables estimation of the number of *Salmonella* cells. This requires a fluorescent strain with highly homogenous fluorescence levels such as *Salmonella* *sifB::gfp*¹¹. Combining the estimated number of *Salmonella* cells for all microcolonies and single cells yields total bacterial tissue loads that are consistent with alternative methods such as plating or flow cytometry of tissue homogenates¹¹. Plating and flow cytometry cannot be done directly from the same tissues because they need to be perfusion-fixed for STP tomography. Instead, they have to be done with additional animals that are not fixed. If the median bacterial loads as determined by the various approaches differ by more than 3-fold, the viability of fluorescent bacteria might be compromised (in case of lower colony-forming units) or some bacteria might have lost the fluorescent reporter construct (in case of higher colony-forming units). Control experiment will be required to identify the source of such discrepancies.

STP tomography provides the localization of bacterial cells within the 3D structure of the infected tissues. The second harmonic signals of collagen provide anatomical landmarks such as arteries and trabeculae. In addition, host cells can be stained *in vivo* by injecting an antibody to surface markers prior to perfusion (Figure 5 and Figure 6). This staining provides additional landmarks for tissue compartments and specific microenvironments including inflammation foci (intracellular markers and some compartments with diffusional barriers such as the splenic white pulp or the brain are not easily accessible suitable for this *in vivo* staining). This approach revealed the splenic white pulp as a tissue compartment that enables long-term survival of *Salmonella* during antimicrobial chemotherapy¹¹.

Finally, *Salmonella* replicating at moderate or slow rates can be identified and localized within the 3D structure of tissues using strains that express *timer*^{bac}, a single cell reporter for replication rate^{11, 15}.

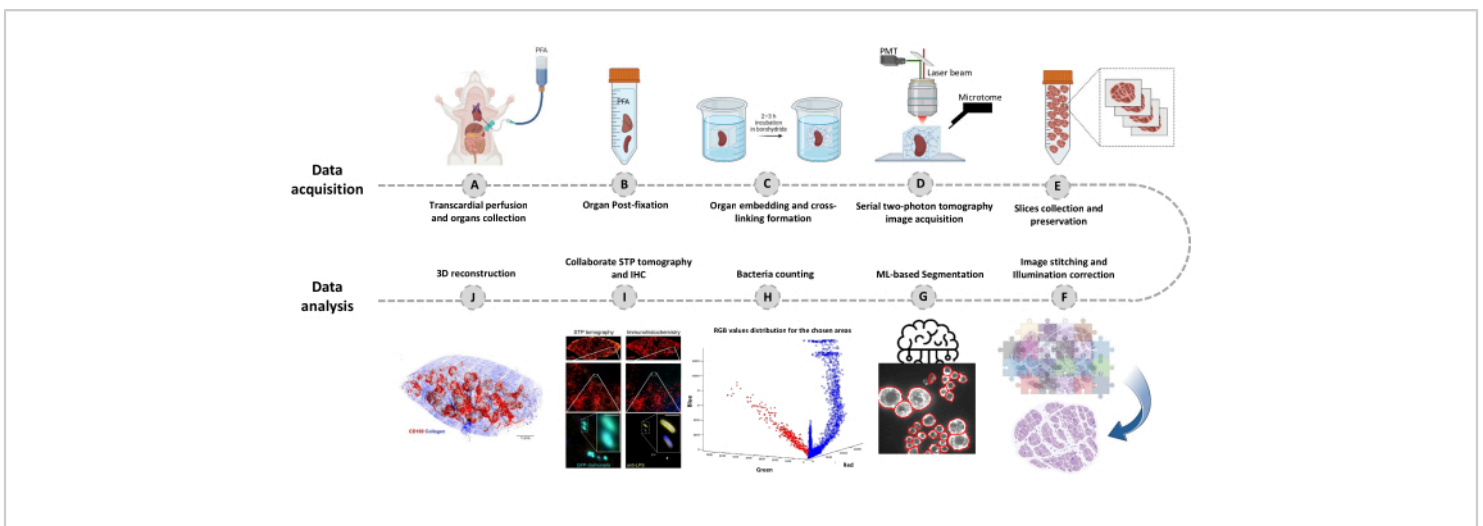


Figure 1: Procedure for whole-organ imaging using serial two-photon (STP) tomography. (A-B) The organ is harvested after transcardial perfusion and stored overnight in 4% paraformaldehyde (PFA) at 4 °C. **(C-E)** The organ is

embedded in oxidized agarose and cross-linked, then the tissue is scanned and sliced using STP tomography. The slices are collected for subsequent immunohistochemistry. (F-J) Computational analysis pipelines for quantifying bacterial numbers, confirmation of fluorescent bacteria, and 3D reconstruction of bacterial positions. [Please click here to view a larger version of this figure.](#)

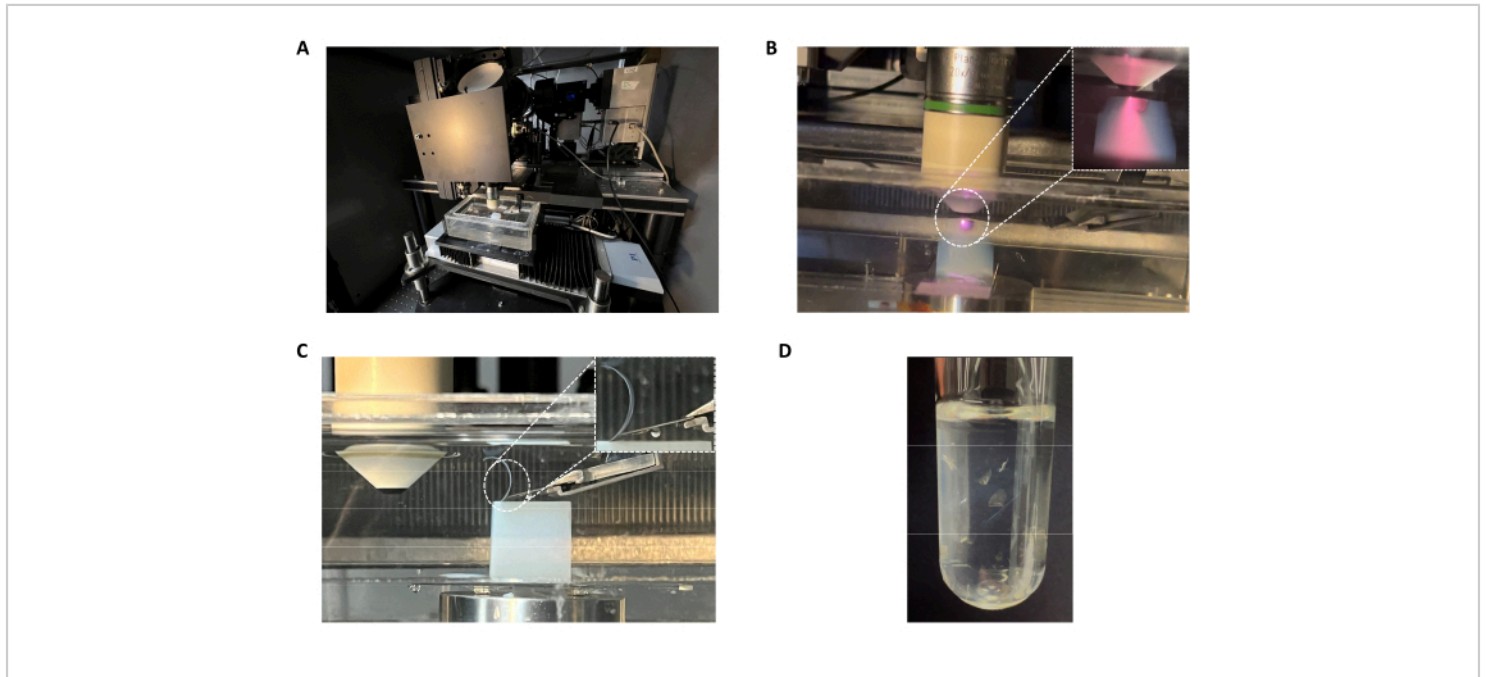


Figure 2: Serial two-photon (STP) tomography setup. (A) Tomograph which incorporates (B) 2-photon imaging with (C) automated serial tissue sectioning. (D) Collected tissue slices for follow-up investigations. [Please click here to view a larger version of this figure.](#)

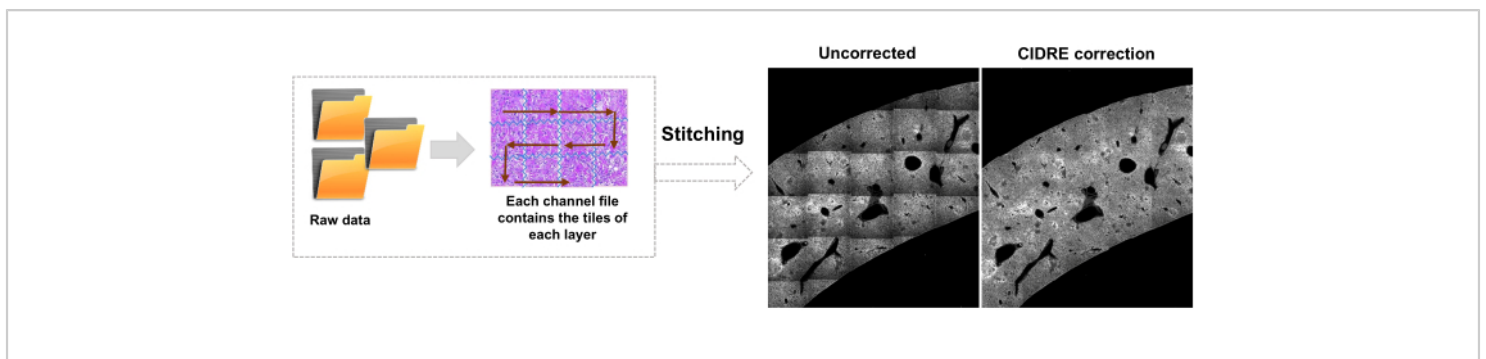


Figure 3: Tile stitching and illumination correction. Tiles are stitched and uneven illumination is corrected for using corrected intensity distributions using regularized energy minimization (CIDRE). [Please click here to view a larger version of this figure.](#)

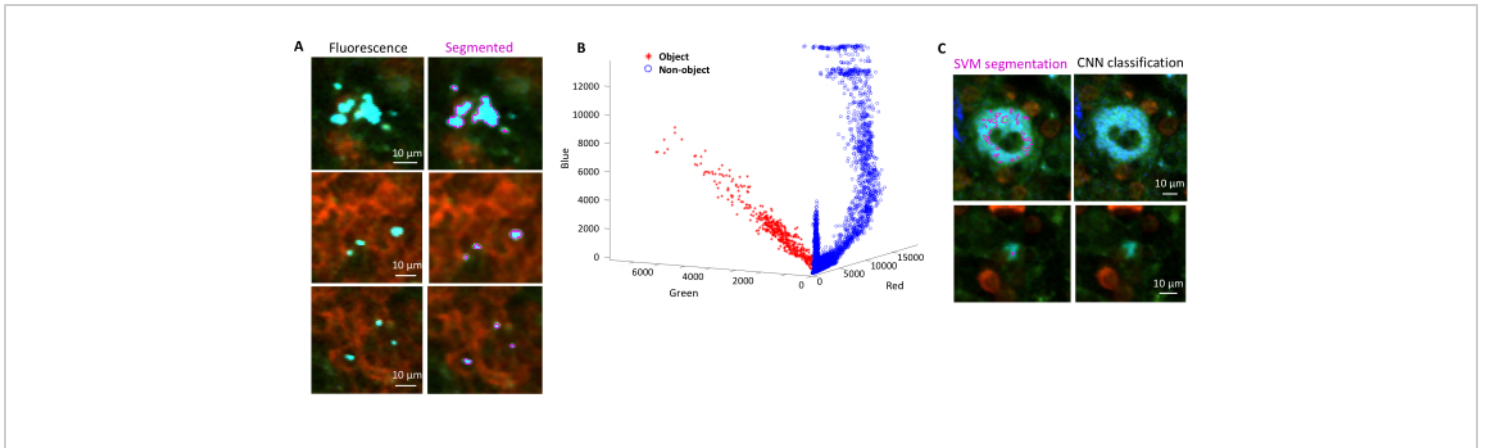


Figure 4: Segmentation of *Salmonella* expressing the green fluorescent protein (GFP) using a Support Vector Machine (SVM) and a Convolutional Neural Network (CNN). (A) Representative images of GFP objects segmented by SVM (left) and corresponding images (right) with regions segmented by SVM (Scale bar: 10 μm). (B) Clustered red-green-blue (RGB) values distribution for the segmented regions. (C) Representative images of non-GFP objects falsely identified by the SVM as bacteria (left). CNN correctly dismisses them as background (right, scale bar: 10 μm). [Please click here to view a larger version of this figure.](#)

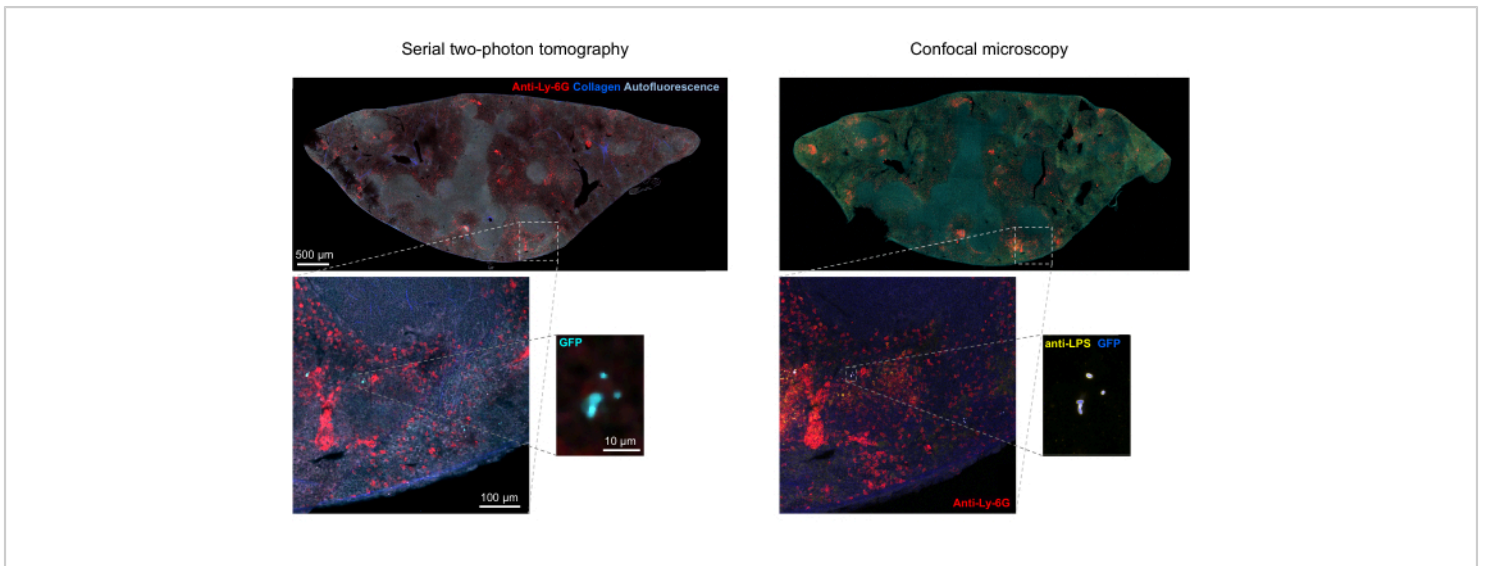


Figure 5: Detection of *Salmonella* expressing the green fluorescent protein (GFP) by tomography and confirmation by immunohistochemistry. Images of the same section acquired by tomography (left) or confocal microscopy after staining with an antibody to *Salmonella* lipopolysaccharide (right). Neutrophils (red) were stained by *in vivo* injection of a PE-labeled anti-Ly-6G antibody prior to perfusion. [Please click here to view a larger version of this figure.](#)

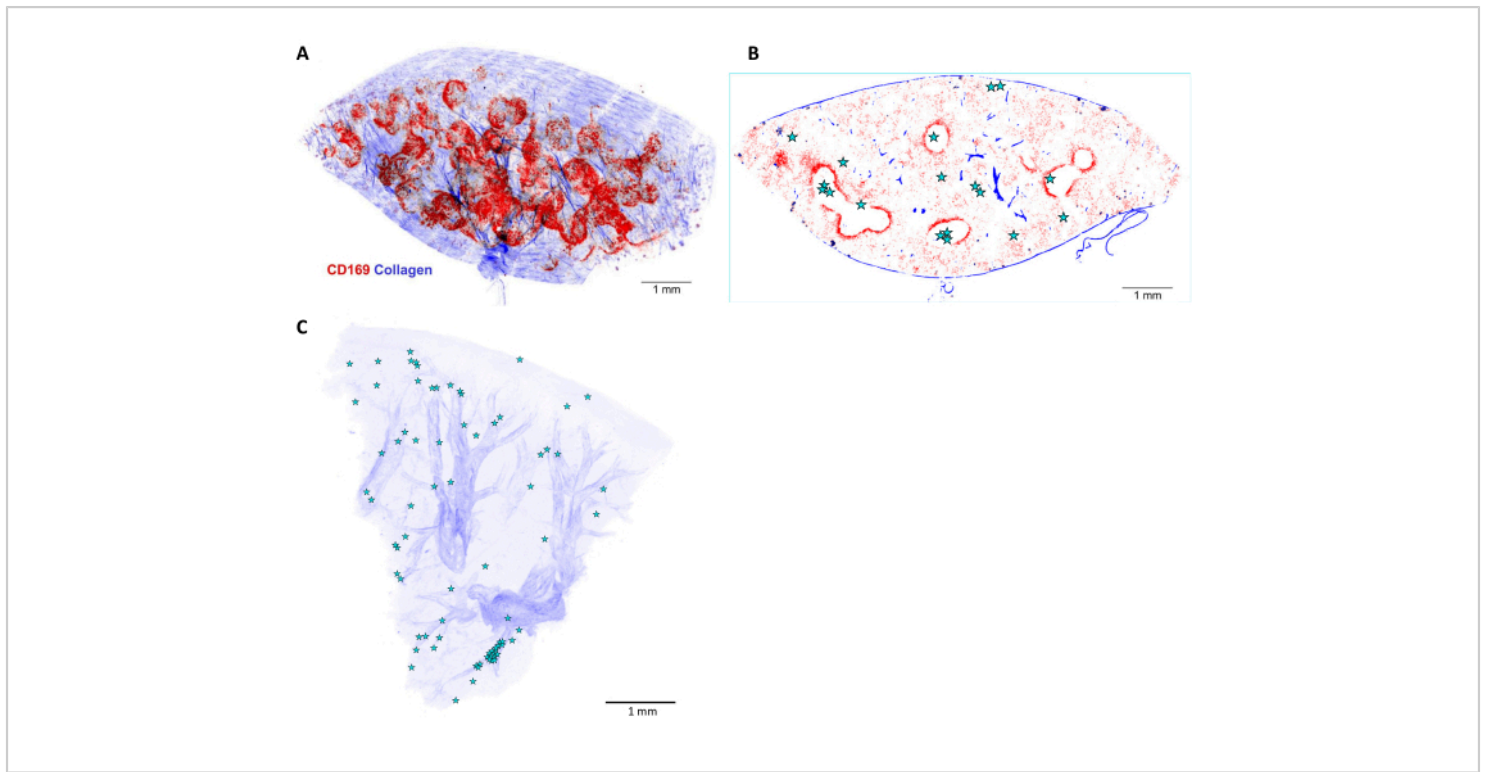


Figure 6: 3D reconstruction and localization of *Salmonella* in infected mouse spleen. (A) Three-dimensional (3D) reconstruction of a 5 mm thick spleen slice and stained *in vivo* before perfusion with anti-CD169 antibody (red). The blue signal represents collagen detected by second harmonics. (B) One optical plane of the 3D stack shown in (A). The positions of *Salmonella* cells or microcolonies are indicated by stars. (C) 3D reconstruction of *Salmonella* positions (stars) in infected liver. The arteries are visible based on their collagen sheaths (blue). Scale bar: 1 mm. [Please click here to view a larger version of this figure.](#)

Discussion

The local tissue context of bacterial pathogens is crucial for determining local host attacks, bacterial adaptations, the local outcome of the host pathogen interactions and antimicrobial chemotherapy, and the individual contributions to overall disease outcome. Imaging micrometer sized bacteria in centimeters size organs has been challenging. Serial two-photon (STP) tomography provides sufficient spatial resolution to detect individual bacterial cells in entire organs, automatized sectioning and imaging, and sufficient throughput (~1 organ per day)¹¹. While host antigens can

be stained *in vivo*, pathogen cells should express suitable fluorescent proteins to ensure comprehensive detection of intracellular pathogen cells. The resulting data sets (0.5-1.5 TeraByte per organ) pose substantial challenges for IT infrastructures for data analysis and storage.

There are several critical steps in this method. First, a pathogen strain with detectable and homogeneous expression of fluorescent protein GFP or YFP is required. Ideally, a chromosomal expression cassette²⁵ is used to minimize fluorescence heterogeneity due to plasmid copy-number variation. Sufficient fluorescence intensity is required

but excessive levels of fluorescent protein should be avoided to avoid fitness impairments of the pathogen²³. Appropriate expression levels can be obtained by selection of an appropriate promoter and fine-tuning of the ribosomal binding site²⁵ or the entire 5' untranslated region (UTR)²⁶. Second, the perfusion fixation should involve an initial wash with buffer to remove as many erythrocytes as possible from the blood circulation. This is particularly critical for spleen and liver (although complete erythrocyte removal from these organs is difficult). Remaining erythrocytes absorb light in the visible part of the spectrum compromising imaging quality²⁷. Third, storage of the fixed tissues in the cryoprotectant is critical to reduce tissue autofluorescence, which is particularly high in inflamed tissues and can overshadow the comparatively weak fluorescence of the pathogen cells¹¹. Fourth, the effective cross-linking of the tissue to the surrounding agarose block is critical for smooth vibratome-cutting without the tissue jumping out of the agarose block. Fifth, fluorescent signals and their identification as pathogen cells must be independently verified using orthogonal approaches such as staining with antibodies to pathogen components (such as lipopolysaccharide for Gram-negative bacteria) and confocal microscopy of the sections retrieved from the tomograph¹¹. Some infected tissues contain auto-fluorescent particles with similar shape and overlapping fluorescence spectra that can be easily misinterpreted as pathogen cells. Sixth, the quantity of pathogen cells within microcolonies should be compared to orthogonal approaches such as confocal microscopy to assess the accuracy. The overall bacterial loads based on these calculations should be verified by comparison to orthogonal approaches such as flow cytometry and plating.

Important modifications of the widely used STP protocol include placing a narrow bandpass filter 510/20 nm in front of photomultiplier 2¹¹, to reduce interference of green-

yellow autofluorescence that is particularly strong in infected and inflamed liver, spleen, and Peyer's patches. The strong autofluorescence and increased light scattering of such organs compared to brain (which dominates other applications of STP) also generates a need for more effective correction for uneven illumination. As another modification, this protocol employs the CIDRE approach²² for this purpose (**Figure 3**) and AI-based segmentation of bacteria. Finally, tissue preprocessing was altered by including an incubation step in cryoprotectant at -20 °C which reduces tissue autofluorescence and thus facilitates detection of small pathogen cells with relatively weak fluorescence¹¹.

Troubleshooting might be necessary if no pathogen signals can be detected, or segmentation yields insufficient sensitivity (too many pathogen cells are missed) or insufficient precision (too many background particles are segmented as pathogen cells). If background tissue autofluorescence is detectable but there are too few pathogen signals, the pathogens might contain insufficient amounts of fluorescent proteins. This can be tested using confocal microscopy of tissue sections from the same infected tissue or flow cytometry of tissue homogenates^{19,28}. Underlying reasons could be insufficient expression levels or instability of the expression cassette. Mitigation strategies could include alternative promoters to drive expression, codon-adaptation of the genes encoding the fluorescent protein for the pathogen species, employment of episomal constructs with higher copy number, or stabilization of expression cassettes by chromosomal integration or balanced-lethal complementation²⁹. The choice of fluorescent protein is also important, but detection is possible with GFP.mut2, mWasabi, YPet, and TIMER^{bac}. If segmentation is inaccurate, this might be caused by too weak pathogen fluorescence which could be addressed as described above, or too high tissue

autofluorescence background. Extensive perfusion of wash solution or prolonged incubation in storage buffer immediately before embedding in the agarose block and tomography might resolve these issues. Finally, sufficient training of the neural network is required for precise classification, but excessive training can lead to overfitting that impairs performance for new samples.

Currently, no other method can image entire organs at sufficient spatial resolution in 3D for detecting individual bacteria. Future improvements in tissue clearing and light-sheet microscopy might achieve similar resolution. This might enable imaging at higher speed and with more fluorescent channels.

An important limitation of STP is the in-plane pixel resolution of $\sim 0.5 \mu\text{m}$ and vertical resolution of 5 to 10 μm , which is insufficient for resolving closely located bacteria, e.g., within a densely packed microcolony. However, it is possible to retrieve tissue sections after tomography for secondary high-resolution confocal microscopy of selected tissue parts. Another limitation of STP is the availability of only three fluorescence channels, which restricts the number of fluorophores that can be imaged simultaneously. Again, secondary analysis of retrieved tissue sections with multiplexing methods can reveal the location and intensity of many more markers for selected tissue parts. This information could be integrated into the overall 3D structure of the surrounding tissue as determined with STP.

In conclusion, this protocol enables detailed investigations of host-pathogen interactions at the local and whole-organ level. The protocol should be easily adaptable to other pathogens (provided they can be obtained as fluorescent strains), other organs, and different host species.

Disclosures

The authors have nothing to disclose.

Acknowledgments

The work was supported by Swiss National Science Foundation 310030_156818, 310030_182315, and NCCR_180541 AntiResist (to DB).

References

1. Bjarnsholt, T. et al. The importance of understanding the infectious microenvironment. *Lancet Infect Dis.* **22** (3), e88-e92 (2022).
2. Azimi, S., Lewin, G. R., Whiteley, M. The biogeography of infection revisited. *Nat Rev Microbiol.* **20** (10), 579-592 (2022).
3. Bumann, D., Cunrath, O. Heterogeneity of *Salmonella*-host interactions in infected host tissues. *Curr Opin Microbiol.* **39** 57-63 (2017).
4. Hofmann, J., Keppler, S. J. Tissue clearing and 3D imaging - putting immune cells into context. *J Cell Sci.* **134** (15), jcs258494 (2021).
5. Blain, R. et al. A tridimensional atlas of the developing human head. *Cell.* **186** (26), 5910-5924.e17 (2023).
6. Ragan, T. et al. Serial two-photon tomography for automated ex vivo mouse brain imaging. *Nat Meth.* **9** (3), 255-258 (2012).
7. Oh, S. W. et al. A mesoscale connectome of the mouse brain. *Nature.* **508** (7495), 207-214 (2014).
8. Kim, Y. et al. Brain-wide maps reveal stereotyped cell-type-based cortical architecture and subcortical sexual dimorphism. *Cell.* **171** (2), 456-469.e422 (2017).

9. Matho, K. S. et al. Genetic dissection of the glutamatergic neuron system in cerebral cortex. *Nature*. **598** (7879), 182-187 (2021).
10. Muñoz-Castañeda, R. et al. Cellular anatomy of the mouse primary motor cortex. *Nature*. **598** (7879), 159-166 (2021).
11. Li, J. et al. Tissue compartmentalization enables *Salmonella* persistence during chemotherapy. *Proc Natl Acad Sci U S A*. **118** (51), e2113951118 (2021).
12. Dogga, S. K. et al. Importance of aspartyl protease 5 in the establishment of the intracellular niche during acute and chronic infection of *Toxoplasma gondii*. *Mol Microbiol*. **118** (6), 601-622 (2022).
13. Cormack, B. P., Valdivia, R. H., Falkow, S. FACS-optimized mutants of the green fluorescent protein (GFP). *Gene*. **173** (1 Spec No), 33-38 (1996).
14. Nguyen, A. W., Daugherty, P. S. Evolutionary optimization of fluorescent proteins for intracellular FRET. *Nat Biotechnol*. **23** (3), 355-360 (2005).
15. Claudi, B. et al. Phenotypic variation of *Salmonella* in host tissues delays eradication by antimicrobial chemotherapy. *Cell*. **158** (4), 722-733 (2014).
16. Ai, H. W., Olenych, S. G., Wong, P., Davidson, M. W., Campbell, R. E. Hue-shifted monomeric variants of Clavularia cyan fluorescent protein: identification of the molecular determinants of color and applications in fluorescence imaging. *BMC Biol*. **6**, 13 (2008).
17. Drobizhev, M., Makarov, N. S., Tillo, S. E., Hughes, T. E., Rebane, A. Two-photon absorption properties of fluorescent proteins. *Nat Methods*. **8** (5), 393-399 (2011).
18. Shaner, N. C. et al. Improved monomeric red, orange and yellow fluorescent proteins derived from *Discosoma* sp. red fluorescent protein. *Nat Biotechnol*. **22** (12), 1567-1572 (2004).
19. Burton, N. A. et al. Disparate impact of oxidative host defenses determines the fate of *Salmonella* during systemic infection in mice. *Cell Host & Microbe*. **15** (1), 72-83 (2014).
20. Wu, J. et al. Transcardiac perfusion of the mouse for brain tissue dissection and fixation. *Bio Protoc*. **11** (5), e3988 (2021).
21. de Olmos, J., Hardy, H., Heimer, L. The afferent connections of the main and the accessory olfactory bulb formations in the rat: an experimental HRP-study. *J Comp Neurol*. **181** (2), 213-244 (1978).
22. Smith, K. et al. CIDRE: an illumination-correction method for optical microscopy. *Nat Methods*. **12** (5), 404-406 (2015).
23. Wendland, M., Bumann, D. Optimization of GFP levels for analyzing *Salmonella* gene expression during an infection. *FEBS Lett*. **521** (1-3), 105-108 (2002).
24. Barat, S. et al. Immunity to intracellular *Salmonella* depends on surface-associated antigens. *PLoS Pathog*. **8** (10), e1002966 (2012).
25. Rollenhagen, C., Sorensen, M., Rizos, K., Hurvitz, R., Bumann, D. Antigen selection based on expression levels during infection facilitates vaccine development for an intracellular pathogen. *Proc Natl Acad Sci U S A*. **101** (23), 8739-8744 (2004).
26. Chen, F., Coccagn-Bousquet, M., Girbal, L., Nouaille, S. 5'UTR sequences influence protein levels in *Escherichia coli* by regulating translation initiation and mRNA stability. *Front Microbiol*. **13**, 1088941 (2022).

27. Weissleder, R. A clearer vision for *in vivo* imaging. *Nat Biotechnol.* **19** (4), 316-317 (2001).
28. Bumann, D. Examination of *Salmonella* gene expression in an infected mammalian host using the green fluorescent protein and two-colour flow cytometry. *Mol. Microbiol.* **43** (5), 1269-1283 (2002).
29. Nakayama, K., Kelly, S. M., Curtiss III, R. J. B. t. Construction of an Asd⁺ expression-cloning vector: stable maintenance and high level expression of cloned genes in a *Salmonella*. vaccine strain. *Nature.* **6** (6), 693-697 (1988).